TECHNICAL PAPER

Effect of wall roughness on performance of microchannel applied in microfluidic device

Junnan Jia[1] · Qinghua Song[1,2] (ID) · Zhanqiang Liu[1,2] · Bing Wang[1]

Abstract

The influence of wall roughness on flow and heat transfer performance in microchannels at low Reynolds number is investigated in this paper. Two sizes of PMMA microchannels are fabricated by microinjection molding and the width is 20 μm and 800 μm respectively. The surface profile of bottom wall is described by the two-dimensional fractal geometry method and it is found there is error within 5% between surface roughness obtained by the fractal geometry method and actual roughness. Then, the effects of dimensionless relative roughness (5–7.5%), fractal dimension (1.5–1.8), aspect ratio (0.025–4) on the flow resistance and heat transfer performance are analyzed by numerical and experimental method respectively. Reynolds number considered here are 10–60. The results show that the better flow performance and heat transfer performance can be obtained with high aspect ratio of rectangular microchannel. However, increasing surface roughness not only increases the heat transfer performance, but also introduces a large flow resistance, which makes the friction coefficient rise sharply. As a result, surface roughness has great influence on the flow and heat transfer performance, and the most suitable surface morphology should be obtained according to the specific application.

1 Introduction

Recently, microfluidic device such as microreactors, micro-mixer and microchannel heat sinks has been developed rapidly and applied in fields of organic chemicals, nanoparticles, biomedical and bioengineering, embedded in a lab-on-chip and cooling system in most electronic devices (Bhagat et al. 2010; Salic 2012; Adham and Mormah 2013; Cortelezzi and Ferrari 2017). A component of microfluidic device, microchannel, which can be defined as an essential and indispensable part with a hydraulic diameter below 1 mm, is embedded in microfluidic devices. Generally, the components of these microdevices are very small, as a result, compared with conventional equipment, there are many advantages including high heat transfer efficient, high sensitivity, easing to mix and integration for microfluidic device (Cheng and Wu 2010; Yeo and Chang 2011). At present, many fabrication processes such as multi-layer tape lithography, 3-D soft lithography, proton beam writing, ultrasonic processing and CO_2 laser cutting technology have been studied in the field of matching and manufacturing of microchannels (Huang and Liu 2010; Singh and Kumar 2014; Al-Shehri and Palitsin 2015; Sackmann and Burlage 2015; Wu and Manz 2015; Chen and Li 2017). The quality and precision of microchannels have been further improved by these processing methods (Chavoshi and Luo 2015; Chen and Zhang 2018).

It can be seen, many studies have concentrated on the surface quality of microchannels. However, it's difficult to control surface quality with such little dimensions and there will be a question that if it is better for fluid flowing through smooth channels than rough channels with regard to heat transfer and flow performance. Furthermore, it was proved that fluid flow through these micro devices would be influenced significant by surface topography and it is

✉ Qinghua Song
  ssinghua@sdu.edu.cn

  Junnan Jia
  jiajunnan123321@163.com

  Zhanqiang Liu
  melius@sdu.edu.cn

1 Key Laboratory of High Efficiency and Clean Mechanical Manufacture, Ministry of Education, School of Mechanical Engineering, Shandong University, Jinan, People's Republic of China

2 National Demonstration Center for Experimental Mechanical Engineering Education, Shandong University, Jinan, People's Republic of China

necessary to investigate the surface roughness effect on fluid flow in microchannels (Taylor et al. 2006; Dai and Li 2014). Some studies (Huang and Liu 2010; Dharaiya and Kandlikar 2013) also found that it may be more useful for mass transfer and heat transfer if there were several roughness elements like micro-protrude, tiny-pits on the surface of micro-channels. In addition, an enhancement of 220% for efficiency of heat transfer was demonstrated when fluid flow through microchannels with herringbone microstructures which was equal to improve surface roughness (Julian and Raphael 2016). As a result, the geometric model of roughness in the microchannels has become a very important factor in the research process. In the literatures, Gauss model method (Yan and Zhang 2015), sinusoidal method (Wang and Zheng 2011) and fractal geometry method (Abuzeid and Al-rabadi 2011) were all used to obtain surface roughness. However, the rough surface described by three dimensional W–M function was proved more scientific and objective (Ji and Zhu 2013). Therefore, the fractal geometric will be used here to gain the surface morphology of microchannels because of the advantages of this method.

The numerical simulation results showed great difference on flow field between microchannels and macrochannels. Many researchers (Demsis and Prabhu 2010; Morini and Yang 2011; Guo and Fletcher 2016) have proposed that rarefaction and slip effect consist in microchannels when the flow medium was gas, which can lead to discontinuity and the traditional method for solving flow field with N–S equation was no longer appropriate. However, with regard to liquid media, the traditional method was still appropriate (Cui and Cui 2015; Kim and Jonathan 2016). In addition, there are also many experimental researches aimed at fluid flowing through a microchannel with roughness surface. The hydrodynamic and thermal performance of three micro-evaporators with different surface roughness was studied by Jafari and Tuba (2016) and the microchannels of evaporators were 700 μm height, 250 μm width. The experimental results for the products of friction factor and Re was obtained where water as working fluid flow through micro-channels with various surface wettability (Yamada and Hong 2011). The Poiseuille and Nusselt number increased as the surface roughness considering the Reynolds number ranged from 150 to 2800 and $Ra = 0.86$, 0.92, 1.02 μm respectively which was investigated by Yuan and Tao (2016). Moreover, five micro-tubes whose diameter varied from 0.2 to 1.0 mm was built to investigate the flow characteristics in microchannels (Zhang and Zheng 2015) and Xanthan gum solution with various concentrations used as working fluid showed an increasing of heat transfer performance (Shojaeian and Karimzadehkhouei 2017).

There are always roughness on the machined surface no matter fabricated by which machining methods and little researches have focus on the influence of surface roughness on the fluid flow through microchannels due to the complex mechanism. This study aims at the effect of surface roughness on flow characteristic and heat transfer performance at low Re with experimental and numerical method respectively in PMMA microchannels which are fabricated by micro-injection molding. The fractal geometry method with more superiority is presented to describe the surface topography and the flow field is solved by CFD code. Furthermore, the range of relative roughness, fractal dimensions D, and aspect ratio α are studied here to analyzed their effect on friction factor f and the average temperature T_{ave} in rectangular microchannels.

2 Fabrication and surface topography description of rectangular microchannels

2.1 Fabrication of PMMA microchannel

Due to its high efficiency and productivity, higher light-admitting quality, higher intensity, higher tenacity, unbreakable and good heat-resistance, good corrosion resistance (Chu and Kamal 2010; Zhang and Gilchrist 2013), micro injection molding is appropriate for mass production of microfluidic chips in recent years. In this study, microfluidic chips designed with two sizes of microchannels are fabricated by micro-injection molding. The microchannel is made of material polymethyl methacrylate (PMMA) due to its high mechanical properties, optical properties, transparency and suitable for mass production. Moreover, the detailed thermophysical parameters of PMMA are 1464 J/kg K for specific heat, 1190 W/m K for thermal conductivity and 1180 kg/m^3 for density. There are three main steps in the forming process of PMMA microfluidic chips. Firstly, a aluminum rectangular micro-pillar which is opposited with microchannel is fabricated by micro-milling, and then combining the micro-pillar with cavity to obtain injection mold. Secondly, taking the mold into injection moulding machine, the preheated PMMA liquid is injected into mold. Then an PMMA substrate with microchannel is formed. In the end, after a work of cleaning, the PMMA substrate is packed with polypropylene (PP) film. The detailed process is shown in Fig. 1.

A microfluidic chip based on PMMA with four microchannels including narrow channels and wide channels named microchannel A and microchannel B respectively are shaped as shown in Fig. 2a. It is 75.5 mm in length, 25.5 mm in width and 1.5 mm in thickness. Moreover, the size of microchannels have the same length which is
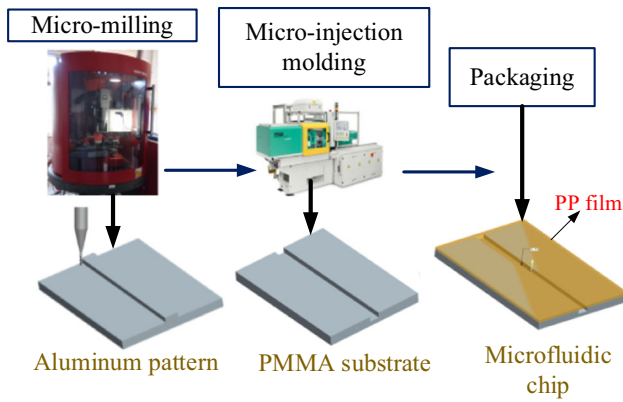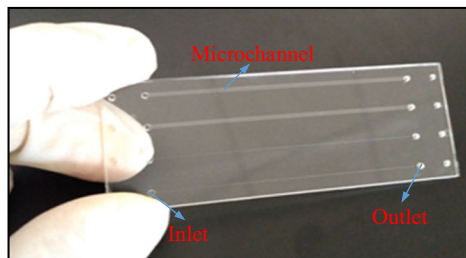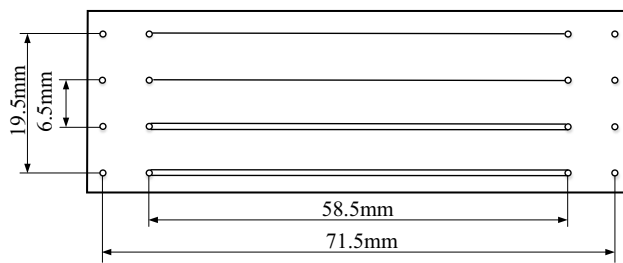
Fig. 1 Diagram of machine process

Fig. 2 Microfluidic chip and dimensional drawing. **a** Microfluidic chip, **b** dimensional drawing

58.5 mm and depth which is 20 μm, the different width which are 800 μm and 20 μm, respectively. The other dimensions are shown as Fig. 2b.

2.2 Surface topography of microchannel

Taylor et al. (2006) pointed that when surface roughness was less than 5%, the influence of roughness on the performance of fluid flow could be neglected in the macro channel, and for microchannel, the influence of roughness on fluid flow could not be neglected. Dai and Li (2014) presented that surface relative roughness 1% can be the critical value of smooth microchannel and a rough microchannel. As a result, fluid flow through these micro devices would be influenced significant by surface topography and it is necessary to investigate the surface roughness effect on fluid flow in microchannels. Due to the

influence of process parameters, such as, injection speed, temperature, quality defects would be induced in the forming process of micro-injection molding (Liu and Song 2009). In our previous studies, process parameter is tightly controlled for obtaining various surface topographies during the forming process of each PMMA substrate. The microchannels with different surface quality would be used to analyse influence of surface roughness on fluid flow and heat transfer in microchannels. In order to observe the microtopography of microchannel clearly, the PMMA substrate with microchannels is placed on the stage of laser microscope (Keyence VK-X series) before packing with PP film. Then, the analysis software VK is applied to distinguish various surface roughnesses and topographies. Various surface topographies are shown in Fig. 3, (a) shows the surface morphology of microchannels A, (b) shows the surface morphology of microchannels B, respectively. It can be seen that the surface morphology of every microchannels are different.

2.3 Characterization of the surface roughness in microchannels by 2-D fractal geometry method

Due to the self-similarity of the roughness on the machined surface, using fractal geometric method to describe the surface topography can gain a more actual model (Ausloos and Berman 1991). To simulate the fractal surfaces, W–M function is used to produce the surface roughness profile. The expression of 2D W–M function is defined as

$$Z(x) = A^{(D-1)} \sum_{\omega=\omega_L}^{\omega_U} \frac{\cos(2\pi\omega x)}{\omega^{(2-D)}} \tag{1}$$

where, $Z(x)$ is the height of surface roughness profile, x is displacement coordinate of surface roughness profile, A is characteristic of the scale coefficient that reflects the scale of $Z(x)$ and it can be defined as

$$A^{D-1} = 2\sigma(\omega_L \cdot \omega_U)^{(2-D)} \sqrt{\frac{2-D}{\omega_U^{4-2D} - \omega_L^{4-2D}}} \tag{2}$$

here, σ is the standard deviation of profile curve, D ($1 < D < 2$) is fractal dimension of the rough surface, ω_L is the lowest cut-off frequency which is related to sampling length L and can be defined as $\omega_L = 1/L$, ω_U is the highest cut-off frequency which can be defined by $\omega_U = 1/(2\delta)$ and δ is resolution of profile which is 0.001 μm here. In this simulation, it is assumed that the upper surface of micro-channels is smooth while the rough bottom surface is described by fractal geometric method. Figure 4 shows the comparison between 2-D fractal models of the bottom surface roughness on the PMMA microchannels and actual bottom roughness when Ra are
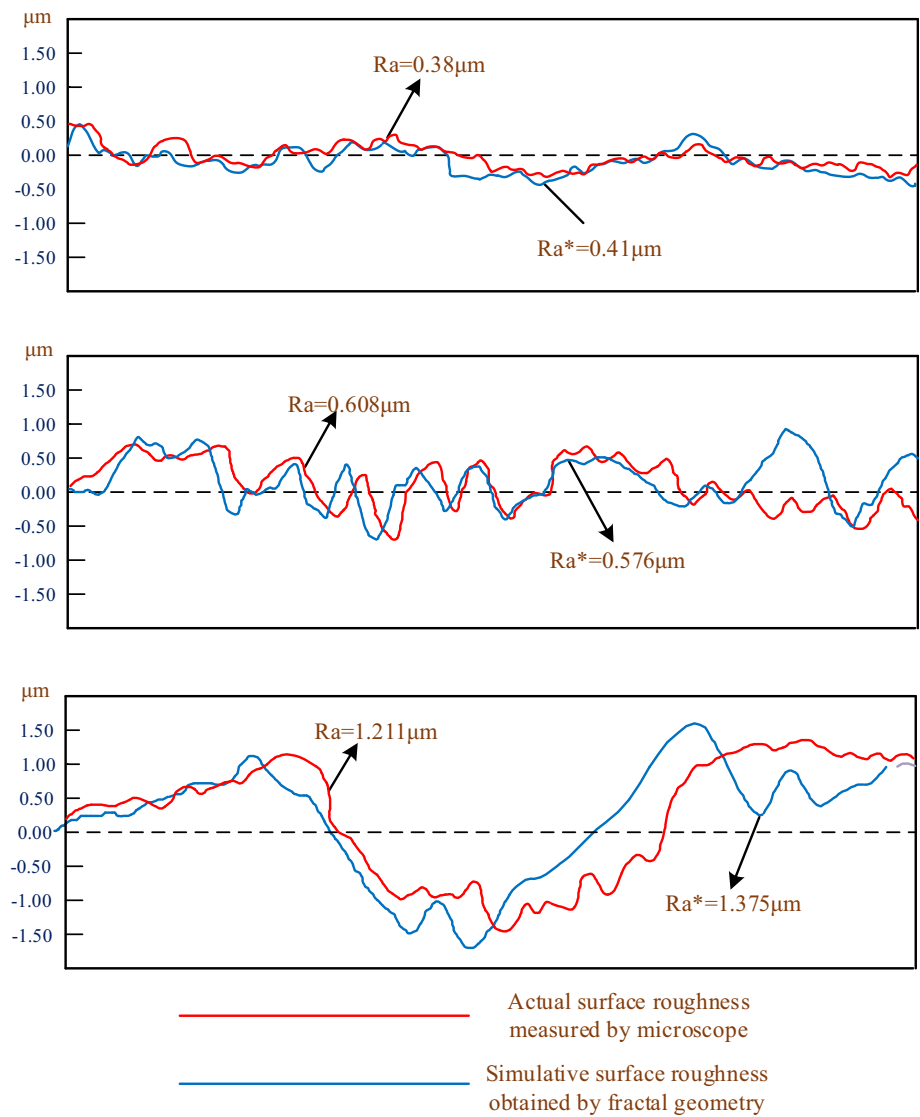
Fig. 3 Surface topographies of microchannels. **a** Microchannels A, **b** microchannels B

(a)

(b)
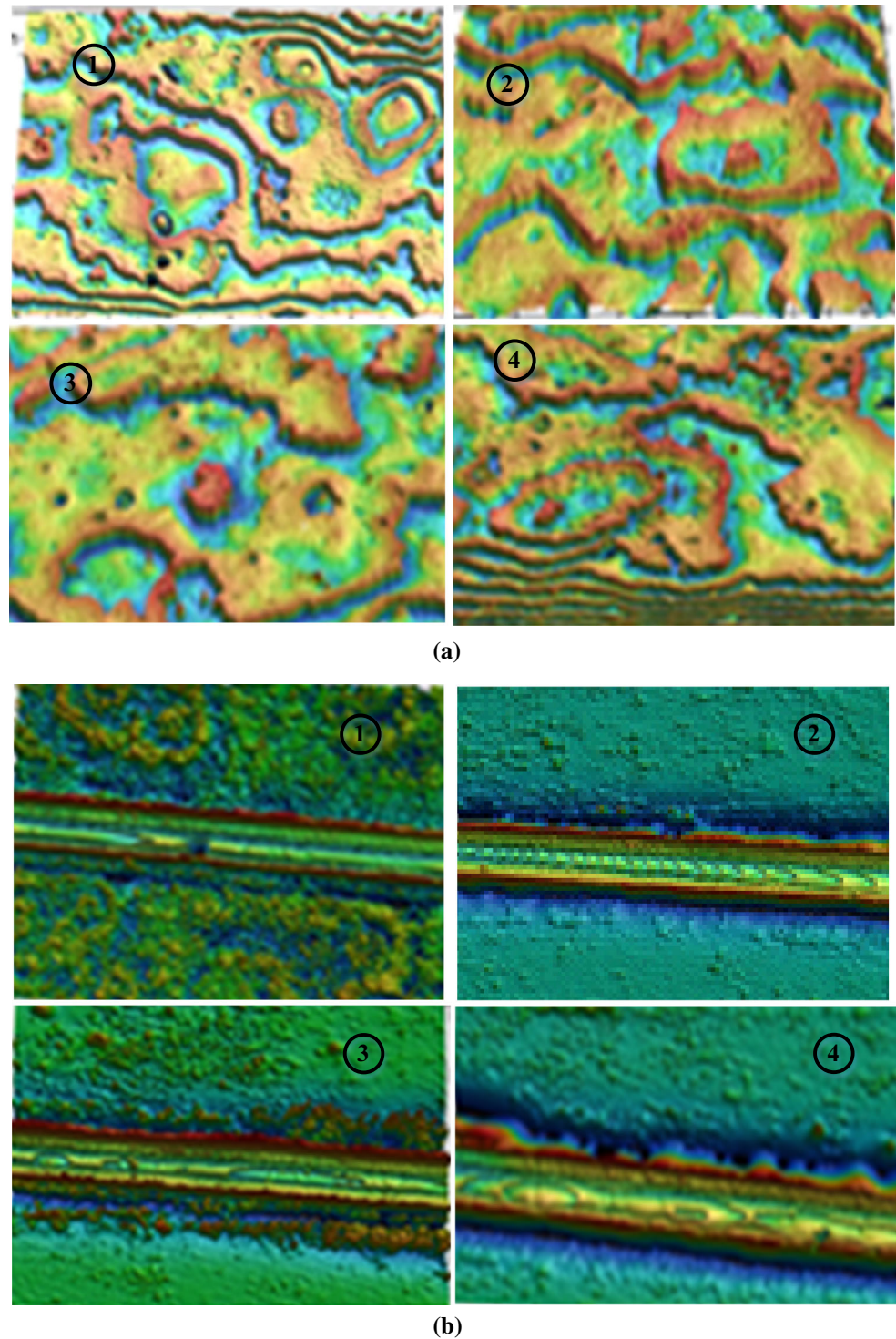
0.380 μm, 0.608 μm and 1.211 μm, respectively. The blue curve is the surface roughness obtained by fractal geometric method, and the red curve is the actual roughness profile obtained by microscope scanning. It can be seen that these two kind of curves have the same shape and the errors of values are within 10%. Therefore, the fractal geometry method can achieve good results when used to simulate the surface morphology of microchannel.

Fig. 4 Comparison of surface profile obtained by fractal method and microscope

Ra=0.38μm

Ra*=0.41μm

Ra=0.608μm

Ra*=0.576μm

Ra=1.211μm

Ra*=1.375μm

⎯⎯⎯⎯⎯ Actual surface roughness measured by microscope

⎯⎯⎯⎯⎯ Simulative surface roughness obtained by fractal geometry

3 Research method for microflow in microchannel

3.1 Experimental study

In order to investigate the effect of surface roughness on flow resistance performance in microchannels, a test bench is built that shown in Fig. 5. Experiments applied to measure the pressure drop of the micro-channel are conducted to validate the numerical results. The test bench is combined with micro syringe pump (Harvard Pump 11 pico plus, USA), pressure sensor (Labsmith uPS01-T116-PKG, USA), PMMA based microfluidic chips fabricated by micro-injection molding technology and data acquisition system. From the drawing of pressure sensor, a close-connected pressure sensor with inlet and outlet of microfluidic can be seen in the diagram,
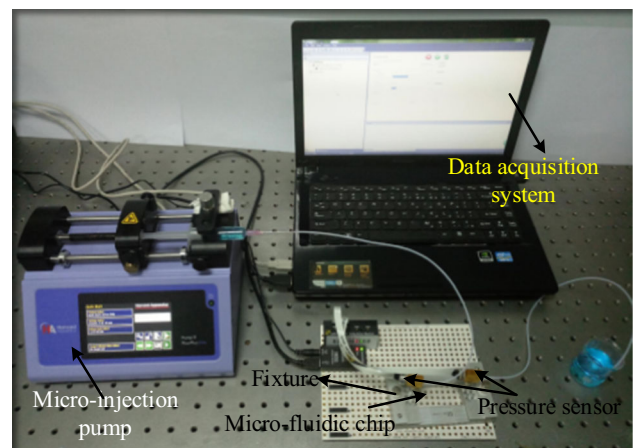

Data acquisition system

Fixture

Pressure sensor

Micro-injection pump

Micro-fluidic chip

Fig. 5 Schematic of the experimental setup

and it is specially designed to decrease the experiment error. As a result, pressure drop between import and export of microchannel obtained from acquisition system is precise due to this system without pipeline loss of on-way resistance. In this work, experiments are carried on to investigate the influence of surface morphology on the hydrodynamic performance. With the help of micro syringe pump, deionized water at ordinary temperature as working fluid flows into micro-channels. The flow rate of pump is correspond to the Re from 10 to 60. Table 1 shows the values of inlet flow rate for the two types of microchannels employed in this experiment. Experimental data which is applied to compared with theoretical results can be obtained by data acquisition system provided by LabSmith Company. Moreover, a multi-measurement average method is applied to decrease experimental error.

3.2 Numerical simulation method

In view of the micron size of channel in microfluidic device, most fluid flowing through these microchannels belong to laminar flow. Moreover, the range of Reynolds number (Re) is between 0.2 and 60 for typical microfluidics system (Geschke 2014). Due to no influences of rarefaction effect and compressibility for liquid flow in this paper, the Navier–Stokes equation is still suitable for this study. In order to investigate the influences of surface roughness on the fluid flow and heat transfer, the CFD programme is used to analyze the fluid field. There are several assumptions such as continuous medium, steady flow, incompressible viscous flow, no slip wall boundary condition and constant wall temperature which are presented to simplify the mathematical model. The mass, momentum and energy conservation equations in differential form for fluid flow are expressed as,

mass equation:

$$\nabla \cdot \vec{v} = 0 \tag{3}$$

momentum equation:

$$\frac{\partial \vec{v}}{\partial t} + \mu \cdot \nabla^2 \vec{v} = -\frac{\nabla P}{\rho} + \nabla \cdot \vec{F} \tag{4}$$

energy equation:

$$\frac{\vec{v}^2}{2} + U + \frac{P}{\rho} = C \tag{5}$$

where ρ is the fluid density, $\vec{v} = (u, v)$ is the velocity vector, μ is the kinematic viscosity, $\vec{F} = (F_x, F_y)$ is the body force vector, P is pressure, U is geopotential energy, C is constant.

Liquid water under the atmospheric pressure used as the working fluid and the physical properties are 998 kg/m^3 for density, 1.005×10^{-3} Pa s for dynamic viscosity, 0.6 W/m K for thermal conductivity and 4182 J/kg K for specific heat. The simulated domain is two-dimension, as shown in Fig. 6, and roughness is only implemented on the bottom wall. The average height of bulges and sags for the roughness profile is defined as e, and dimensionless relative roughness ε is obtained by,

$$\varepsilon = \frac{e}{D_h} \tag{6}$$

where D_h is hydraulic diameter of rectangular microchannels that is defined as a ratio of four times the area to the perimeter for the cross section of microchannels.

An inlet velocity boundary condition is imposed at the left side of the model and the outlet pressure boundary condition is imposed at the right side. Numerical simulation is carried out around water fluid through microchannels under different relative surface roughness that ε changed from 5 to 7.5% and different aspect ratio of microchannels. Detailed data simulated in this paper are shown in Table 2. Reynolds number Re is a dimensionless number representing the ratio of inertial force to viscous force of fluid, and the value for simulation in this paper is 10-60. Furthermore, Re is defined as

$$\text{Re} = \frac{\rho u D_h}{\mu} \tag{7}$$

where ρ is the fluid density and μ is dynamic viscosity, D_h represents the hydraulic diameter and u is the inlet velocity.

In order to improve and perfect the numerical simulation, several boundary conditions are needed. At the inlet of microchannels, temperature is set up for $T_{in} = 300$ K, the inlet velocity in the direction x can be obtained from Eq. (7) and the inlet velocity in the direction y is 0. At the outlet of microchannels, the pressure outlet is applied that $P_{out} = 0$. At the bottom wall, the constant wall heat flux 100 W/cm^2 is imposed on the bottom surface of channels. The top wall are assumed as adiabatic walls where $\left(\frac{\partial T}{\partial n}\right)_{u,v} = 0$.

Nusselt number is a standard number which represents the intensity of convection heat transfer and defined as

Table 1 Volume flow rate used in the experiments

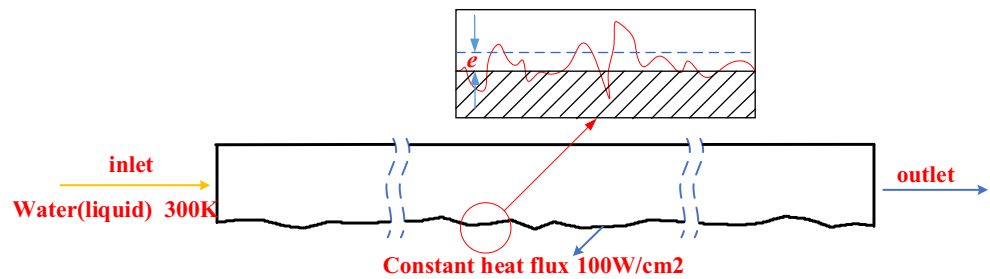| Microchannel	1	2	3	4	5	6
A (10^{-2} ml/min)	2.14	4.29	6.43	8.58	10.72	12.87
B (10^{-1} ml/min)	4.40	8.80	13.20	17.60	22.00	123.55

Fig. 6 Diagram of 2-D simulated domain

Table 2 Detailed data simulated in this paper

	Case 1 (microchannel A)	Case 2	Case 3 (microchannel B)	Case 4	Case 5	Case 6	Case 7
Aspect ratio α	1	0.2	0.025	0.05	2	0.4	4
Height (μm)	20	20	20	40	30	40	80
Width (μm)	20	100	800	800	20	100	20
Hydraulic diameter d_h (μm)	20	33.3	39	76.2	24	57.1	32

$$Nu_{ave} = \frac{hd_h}{\eta_l} \qquad (8)$$

where d_h represents hydraulic diameter, η_l means the thermal conductivity of fluid, h is the heat transfer coefficient and described as

$$h = \frac{q}{T_b - T_f} \qquad (9)$$

where q represents the heat flux that applied in the bottom surface, T_b is the average temperature of the bottom surface and T_f is the temperature of fluid.

In the end, for analyzing the flow resistance in the microchannels, Darcy friction factor is used to represent hydraulic resistance

$$f = \Delta P \times \frac{D_h}{L} \times \frac{2}{\rho v_{ave}^2} \qquad (10)$$

where ΔP is the pressure difference between inlet and outlet of microchannels, D_h is equivalent diameter of channel, L is the length of model domain, ρ is the density of flow fluid, v_{ave} represents the average velocity.

4 Results and discussion

4.1 Effect on hydrodynamic performance

The influence of the surface roughness of the bottom surface on the flow resistance in microchannels is studied by experimental and numerical methods. And the pressure drop obtained by experiment in different cases is shown in Table 3. It can be seen the pressure drop increases with the

surface roughness. The friction factor f which can be derived from Eq. (8) is used to evaluate the flow resistance in microchannels. The Fig. 7a, b show the friction factor f various with Reynolds number Re at different relative roughness 5%, 5.5%, 6.5% for microchannel A and microchannel B respectively. It can be indicated that with the increase of Re, the friction factor f decreases rapidly and this conclusion can also be confirmed by Zhang and Zheng (2015). Moreover, the friction factor f increases with the increase of relative roughness ε, and when ε increases from 5 to 5.5%, f increases about 100%, ε increases from 5.5 to 6.5%, f increases about 15%. Therefore, the friction factor f does not increase linearly with the increase of relative roughness ε. Compared with the experimental and numerical results, the friction factor obtained by experiment is always lager than results of numerical simulation due to the existence of pipeline loss and other uncertain factor during the experiment and the error is kept within 5%. Therefore, the results obtained by these two methods are in good agreement and the numerical method used in this paper is feasible.

Figure 8a represents the near-wall streamlines on the rough surface in Case 7 microchannels with relative roughness varies from 5 to 7.5% when the Reynolds number Re is 60, and Fig. 8b shows the partial enlarged drawing of vortex. From the drawing (a), disturbance near the bottom wall grows with the increasing of relative roughness obviously. When the relative roughness ε is 5%, the fluid flow through the microchannels is smooth and stable. However, when ε increases to 5.5%, several vortex begins to appear in the depression of the rough bottom surface. Moreover, with the increase of relative roughness, the vortices become more and larger. Meanwhile, the

Table 3 Data of pressure drop of microchannel in different cases

Pressure drop (Pa)	Microchannel A			Microchannel B		
	$\varepsilon = 5\%$	$\varepsilon = 5.5\%$	$\varepsilon = 6.5\%$	$\varepsilon = 5\%$	$\varepsilon = 5.5\%$	$\varepsilon = 6.5\%$
Re = 10	10,029	21,976	24,173	13,351	24,098	29,057
Re = 20	22,749	46,857	49,491	29,362	51,079	60,534
Re = 30	36,473	80,852	83,906	47,184	78,966	91,101
Re = 40	60,346	110,796	121,971	67,727	107,519	127,672
Re = 50	90,819	144,713	150,202	83,039	141,272	168,070
Re = 60	94,866	179,670	186,857	103,331	171,045	173,430
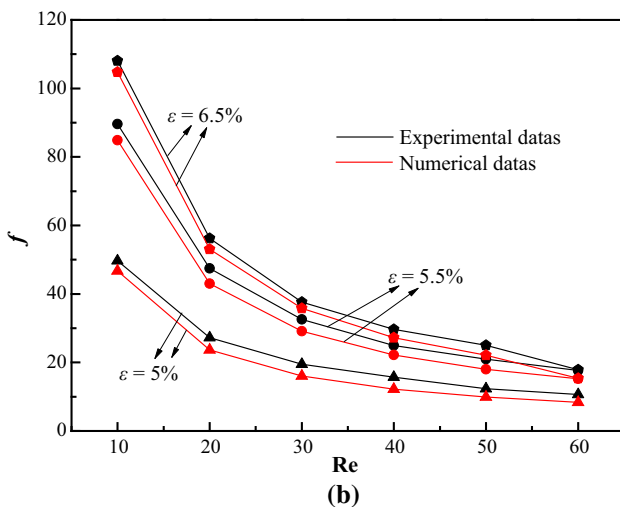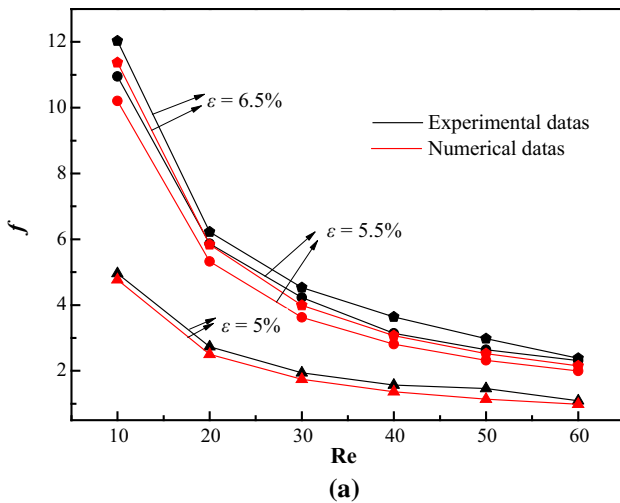
Fig. 7 Comparison between experimental and numerical results for the friction factor f various with Re at different relative roughness ε **a** microchannel A, **b** microchannel B
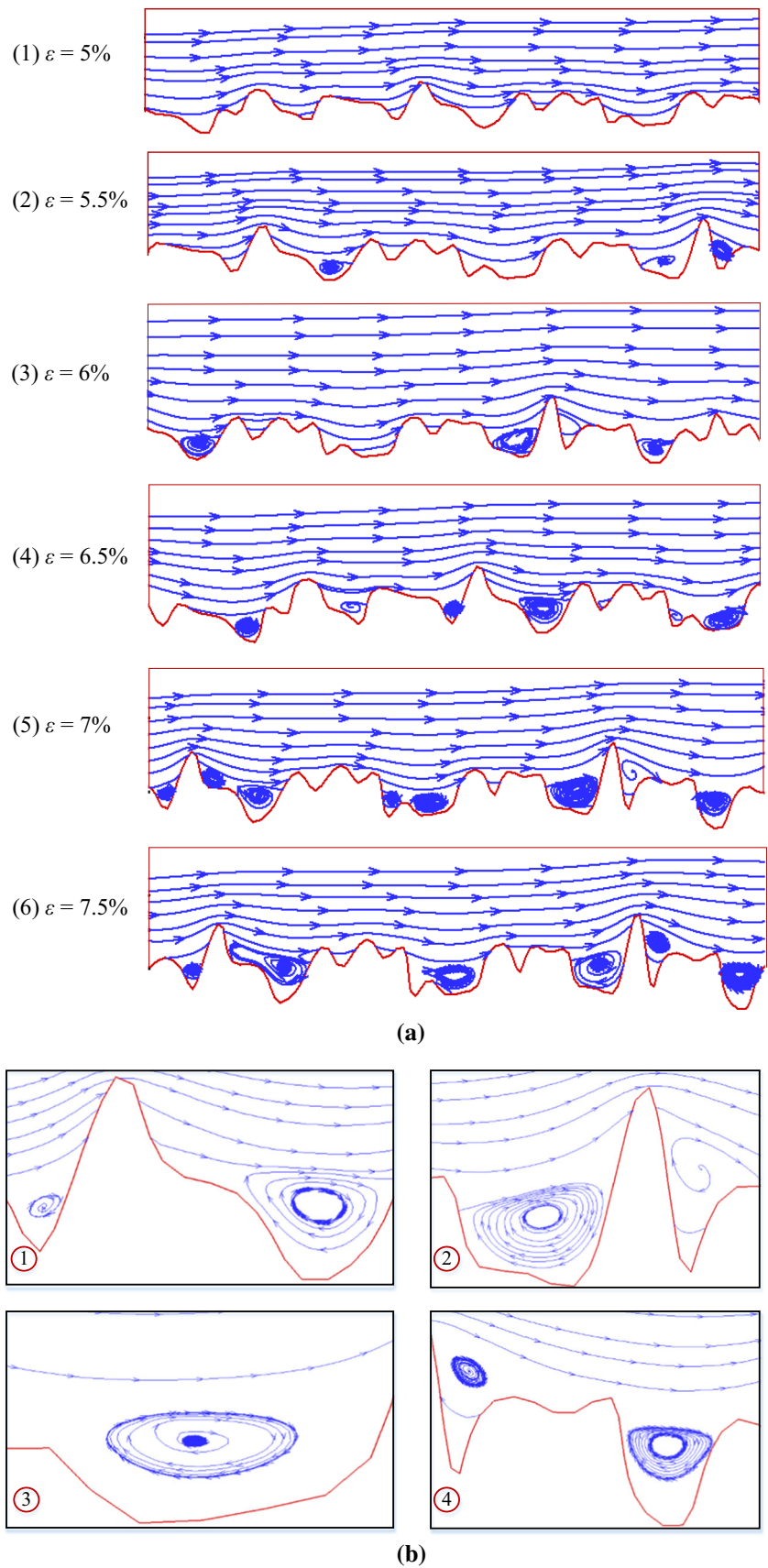
separation of boundary layer is observed at the bottom wall. In addition, separation of boundary layer only can be observed behind the surface micro-convexities. The existence of these vortices makes the fluid flow in the microchannels begin to be disturbed and unstable that increasing flow resistance. Figure 9 shows the velocity

contours in cases 1 for Re = 10, $\varepsilon = 5\%$ and Re = 60, $\varepsilon = 5\%$ respectively. It can be seen that the lowest value of velocity of the whole field appears at the rough wall in microchannels. Therefore, it is also proved that the flow resistance is introduced by wall roughness which also obstructs the fluid flow in microchannels. Consequently, in the micro-channels the flow can be disturbed due to the existence of roughness in the wall, and when the roughness in the wall reaches to a certain degree, a separation of boundary layer can be found near wall. Therefore, there is a larger flow loss with the increasing of the wall roughness.

The influence of fractal dimensions D on friction factor f is presented in Fig. 10. It can be seen that f increases obviously with the increase of D which is various from 1.5 to 1.8. For the small Re, the friction factor f increases with fractal dimensions D exponentially and when Re increases to 60, the value of f decreases. When D increases, the increasing of f becomes relatively slow. The value of f for $D = 1.75$ is about three times higher than $D = 1.5$. After that, as the fractal dimension D continues to increase, the friction factor f no longer increases significantly. It is showed that surface roughness can be enlarged with the increase of D which introduced much resistance when the fluid flow through the microchannels and the friction factor f would be increased. However, there is a top limit for the increasing of surface roughness caused by the fractal dimension. Therefore, with the increase of D, the increasing amplitude of f decreases gradually, and the friction factor f would be constant.

Figure 11 shows the variation of the friction factor f with the aspect ratio α of microchannels when the relative roughness ε is 5%. It can be indicated that f decreases gradually with the increase of α of microchannels and the value of f for $\alpha = 0.025$ is 200% less than $\alpha = 0.4$. There are also two areas with significant difference for the friction factor f namely $\alpha > 1$ and $\alpha < 1$. For microchannels with $\alpha < 1$, the values of f are various from 10 to 50 and decreases obviously with the increase of Re. Meanwhile, for $\alpha > 1$, the values of f contains about 5 and could not change with Re significantly. When the height is low and the width is large in microchannel with smaller aspect ratio, a larger blockage would be produced in the flow

Fig. 8 Near-wall streamline of microchannel case 7 at Re = 60 **a** streamlined for ε changed from 5 to 7.5% respectively, **b** the partial enlarged drawing of vortex
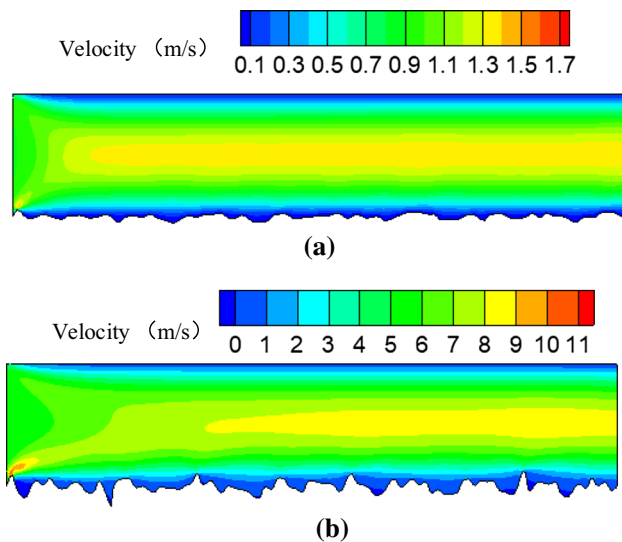
(1) $\varepsilon = 5\%$

(2) $\varepsilon = 5.5\%$

(3) $\varepsilon = 6\%$

(4) $\varepsilon = 6.5\%$

(5) $\varepsilon = 7\%$

(6) $\varepsilon = 7.5\%$

(a)

(b)

Velocity （m/s）

0.1 0.3 0.5 0.7 0.9 1.1 1.3 1.5 1.7

(a)

Velocity （m/s）

0 1 2 3 4 5 6 7 8 9 10 11

(b)

Fig. 9 Contours of velocity in microchannels **a** Re = 10, ε = 5% for case 1, **b** Re = 60, ε = 7.5% for case 1
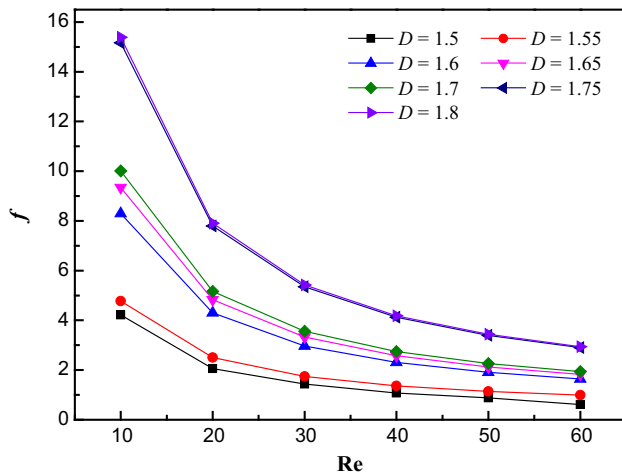
Fig. 10 Friction factor *f* related to Re at different fractal dimensions *D*

Fig. 11 Friction factor *f* related to Re at different aspect ratio α

Fig. 12 Friction factor *f* related to Re at different relative roughness ε

process which is not conductive to fluid transmission due to the larger friction factor. As a result, for cases of α in this study, the lager aspect ratio would grow the lower friction factor *f* which means the better flow performance.

When the aspect ratio α = 1, the friction factor *f* varies with relative roughness ε of bottom surface in microchannel is shown in Fig. 12. It can be indicated that flow disturbance increases with Re varying from 10 to 20, and *f* decreases sharply by 50% with the decrease of flow resistance. Then, when Re increases from 20 to 60, the flow in microchannels tends to be stable and *f* decreases slightly. Furthermore, the friction factor *f* increases with the relative roughness ε of the bottom surface in microchannels which causes a larger resistance of fluid flow (Cui and Cui 2015). However, the increase of *f* is not linear. The value of *f* for
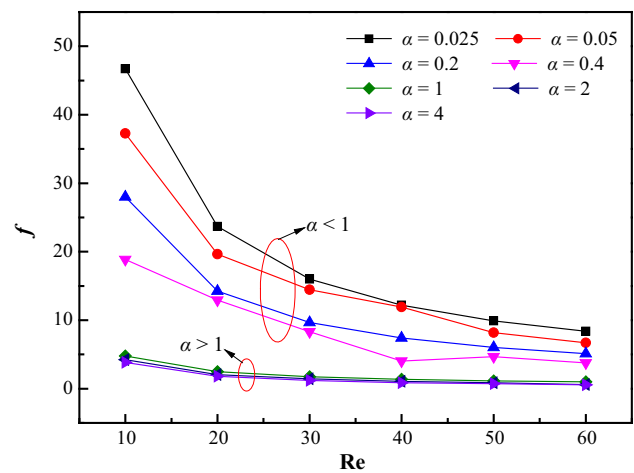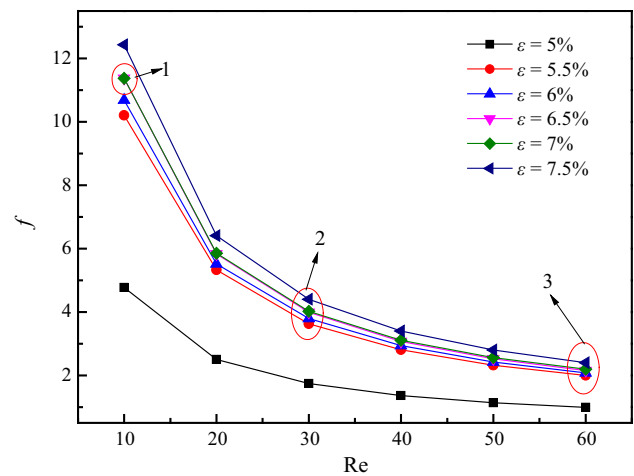
ε = 5.5% is 100% larger than that is 5% and with the relative roughness ε continues to increase, *f* increases more and more slowly and there is no large difference in friction factor *f* for ε = 6.5% and ε = 7% as shown in region 1 of the diagram. Moreover, for a small Re, increase ε from 5.5 to 7.5%, *f* can be still increased by about 30%. For microflow with higher Re, *f* would no longer increases significantly when the relative roughness ε rises from 5.5 to 7.5% which can also be seen from the regions 2 and 3 in Fig. 13. Therefore, the flow resistance caused by surface roughness could not always increase with the increase of relative roughness of bottom surface in microchannels.

4.2 Effect on thermal performance

Heat flux with constant rate of 100 W/cm² is applied to the bottom surface of the microchannels which cause the increase of surface temperature. Then, when cold fluid flow through the microchannels, the heat of bottom surface can
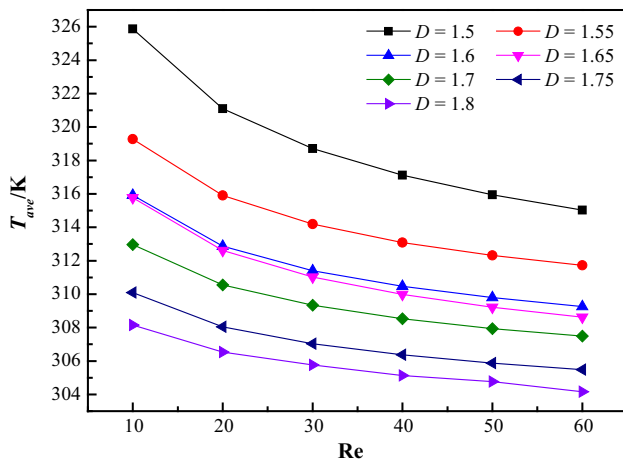
Fig. 13 T_{ave} varied with Re at different fractal dimensions D

be taken away and the bottom surface temperature is reduced. Finally, the heat transfer capacity of different microchannels can be evaluated by analyzing the mean temperature T_{ave} of bottom surface. Figure 13 shows the effect of fractal dimension on the average bottom surface temperature T_{ave} in microchannel. It can be seen from the diagram that the fractal dimension has a great effect on the T_{ave}. For micro-channels with different fractal dimensions, the increase of Re always makes the T_{ave} drops rapidly considering that the increase of Reynolds number Re, that is, the increase of inlet velocity of fluid, enhances the flow disturbance that causes the increase of convection heat transfer coefficient of the fluid and strengthens the heat transfer. Figure 14 reveals several examples of temperature contours, and it can also be seen from Fig. 14, the maximum temperature of the bottom wall decreases with the
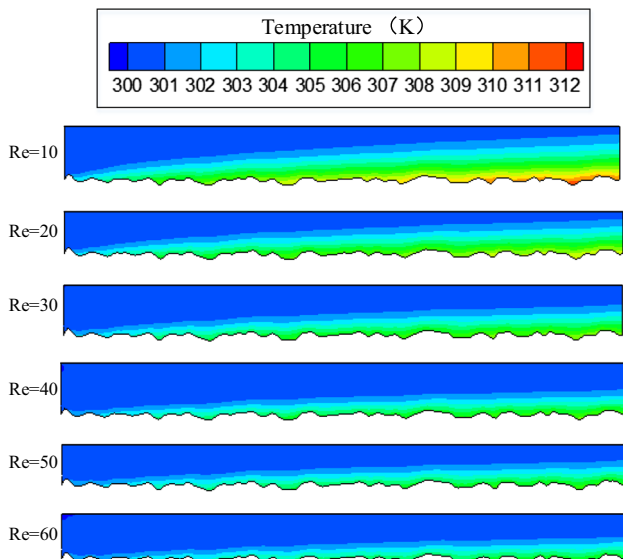
increase of Re. On the other side, with the increase of fractal dimension D, the T_{ave} decreases gradually and when the fractal dimension increases from 1.5 to 1.8, T_{ave} decreases 34%. It is caused by the increase of fractal dimension which leads to the increase of the roughness of the bottom surface that enlarging the contact area between the fluid and the solid bottom surface and strengthening the heat transfer which makes the decrease of T_{ave}.

The variation of T_{ave} with the aspect ratio α of microchannels when the relative roughness is 5% is shown in Fig. 15. It can be seen from the figure that T_{ave} decreases with the increase of aspect ratio α. For α changing from 0.025 to 0.2, the decrease of the average bottom surface temperature T_{ave} is up to 30% due to the doubled increasing of α. When α is more than 1, it increase in parity, that is $\alpha = 1$, $\alpha = 2$, $\alpha = 4$ respectively and the decrease of T_{ave} is not much, but is still containing decreasing. The higher aspect ratio makes increasing the contacted surface area between fluid and solid wall, that is, the heat transfer surface area increases. Therefore, the heat transfer in microchannel is enhanced, and the average bottom surface temperature T_{ave} decreases faster. It can be concluded that the thermodynamic performance of microchannels can be enhanced by the increase of the aspect ratio.

Figures 16 and 17 show the variation of the T_{ave} and Nu_{ave} with relative surface roughness ε when the aspect ratio is 1 respectively. It can be seen with the increase of ε the bottom surface temperature T_{ave} decreases and Nu_{ave} increases which revealed the optimization of heat transfer performance. Moreover, region 1 and 2 in Fig. 16 is quite different in the value of T_{ave}. When ε increases from 5 to 6%, the average temperature T_{ave} drops slowly, however, with ε increasing to 6.5%, the decrease of T_{ave} is twice higher than before. It can also be seen from region 1 that with the relative roughness increasing from 6.5 to 7.5%, the
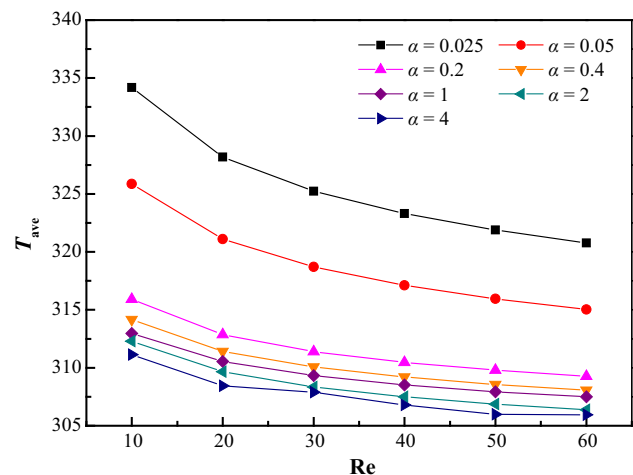

Fig. 14 Contours of temperature in microchannels for Re = 10–60, ε = 7.5% of case 1

Fig. 15 The bottom surface temperature T_{ave} related to Re at different aspect ratio α
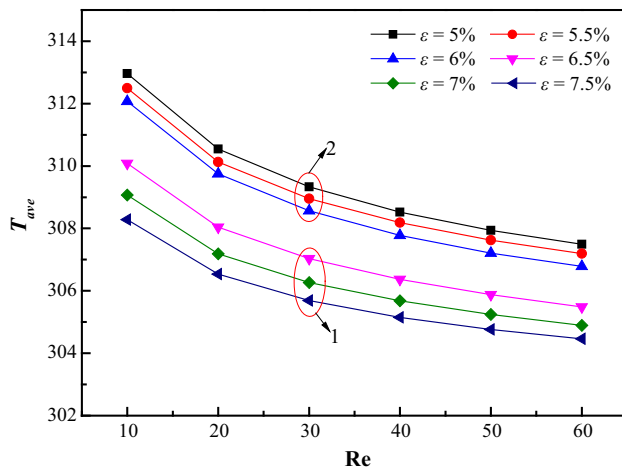
Fig. 16 The bottom surface temperature T_{ave} related to Re at different relative roughness ε
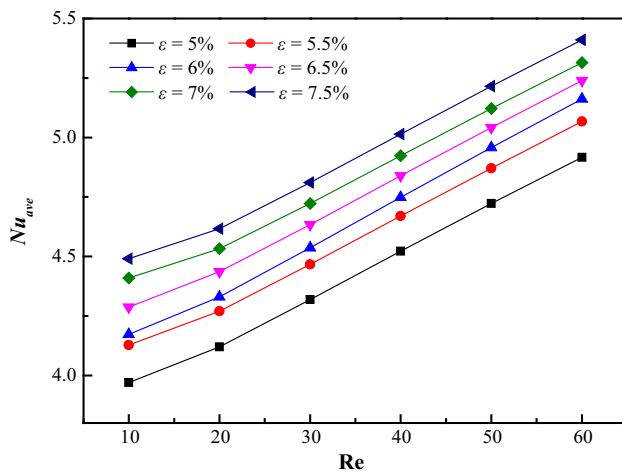

Fig. 17 The average Nusselt number Nu_{ave} related to Re at different relative roughness ε

decrease of mean bottom temperature is still obvious and up to 5.5%. Therefore, with the increase of surface roughness, the average temperature T_{ave} on the bottom surface could decrease continuously. It can be summarized that the surface contact area between fluid and the solid wall could be increased with the relative surface roughness ε that increasing the heat transfer area and enhancing the heat transfer in the microchannel (Kandlikar and Joshi 2003).

5 Conclusions

In this paper, microchannel based on PMMA was fabricated by microinjection molding method. The geometric profile of bottom surface of microchannel was built by fractal geometry methods and the flow field was solved to

research the influence of surface roughness on flow and heat transfer performance at low Re. Moreover, the effects of relative roughness ε, fractal dimensions D, and aspect ratio α on friction factor f and the average temperature T_{ave} in microchannels was analyzed. The detailed conclusions are as follows:

1. Fractal geometry theory is an appropriate and efficient method to build surface roughness, there is small error between fractal model and actual roughness.
2. With the increase of flow velocity, the disturbance of the flow is increased which makes enhancing of the heat transfer performance in microchannel, meanwhile accompanied by the increasing of flow resistance.
3. Surface roughness in microchannels has a great influence on the flow and heat transfer performance. More flow resistance is introduced by bottom wall roughness in microchannels and heat transfer performance is also enhanced sharply.
4. Microchannels with high aspect ratio have better flow and heat transfer performance.

Compliance with ethical standards

Conflict of interest The authors declare that they have no conflict of interest.

References

Abuzeid OM, Al-rabadi AN (2011) Recent advancements in fractal geometric-based nonlinear time series solutions to the micro-quasistatic thermoviscoelastic creep for rough surfaces in contact. Math Probl Eng 10:1155–1185

Adham AM, Mormah GN (2013) Thermal and hydrodynamic analysis of microchannel heat sinks: a review. Renew Sustain Energy Rev 21:614–622

Al-Shehri S, Palitsin V (2015) Fabrication of three-dimensional SU-8 microchannels by proton beam writing for microfluidics application: fluid flow characterisation. Nuclear Instrum Methods 348:223–228

Ausloos M, Berman DH (1991) A multivariate Weierstrass–Mandelbrot function. ASME J Tribol 113:1–11

Bhagat AS, Bow H, Hou HW (2010) Microfluidics for cell separation. Med Biol Eng Comput 48:999–1014

Chavoshi SZ, Luo XC (2015) Hybrid micro-machining processes: a review. Precis Eng 41:1–23

Chen XY, Li TC (2017) Surface roughness study on microchannels of CO_2 laser fabricating PMMA-based microfluidic chip. World Sci 1750017:1–7

Chen XY, Zhang L (2018) Review in manufacturing methods of nanochannels of bio-nanofluidic chips. Sens Actuator B Chem 254:648–659

Cheng S, Wu ZG (2010) Microfluidic electronics. Lab Chip 12:2782–2791

Chu JS, Kamal MR (2010) Characterization of microinjection molding process. Polymer Eng Sci 50:1214–1225

Cortelezzi L, Ferrari S (2017) A scalable active micro-mixer for biomedical application. Microfluid Nanofluid 21:31–47

Cui J, Cui YY (2015) Effects of surface wettability and roughness on the heat transfer performance of fluid flowing through microchannels. J Energies 8:5704–5724

Dai BM, Li MX (2014) Effect of surface roughness on liquid friction and transition characteristics in micro- and mini-channels. Appl Therm Eng 67:283–293

Demsis A, Prabhu SV (2010) Influence of wall conditions on friction factor for flow of gases under slip condition. Exp Therm Fluid Sci 34:1448–1455

Dharaiya VV, Kandlikar SG (2013) A numerical study on the effects of 2D structured sinusoidal elements on fluid flow and heat transfer at microscale. Int J Heat Mass Transf 57:190–201

Geschke O (2014) Microsystem engineering of lab-on-a-chip device. Clin Chem 12:2470–2471

Guo ZY, Fletcher DF (2016) Numerical simulation of annular flow hydrodynamics in microchannels. Comput Fluids 133:90–102

Huang YG, Liu SB (2010) Surface roughness analysis and improvement of PMMA-based microfluidic chip chambers by CO_2 laser cutting. Appl Surf Sci 256:1675–1678

Jafari R, Tuba OO (2016) Experimental investigation of surface roughness effects on the flow boiling of R134a in microchannels. Exp Therm Fluid Sci 79:222–230

Ji CC, Zhu H (2013) Fractal prediction model of thermal contact conductance of rough surfaces. Chin J Mech Eng 26:1–9

Julian M, Raphael B (2016) Significant heat transfer enhancement in microchannels with herringbone-inspired microstructures. Int J Heat Mass Transf 95:755–764

Kandlikar SG, Joshi S (2003) Effect of surface roughness on heat transfer and fluid flow characteristics at low Reynolds numbers in small diameter tubes. Heat Transf Eng 24:4–16

Kim JH, Jonathan PR (2016) Delayed lubricant depletion on liquid-infused randomly rough surfaces. Exp Fluids 57:81–89

Liu Y, Song MC (2009) Quality defects and analysis of the microfluidic chip injection molding. Mater Sci Forum 628:417–422

Morini GL, Yang YH (2011) A critical review of the measurement techniques for the analysis of gas microflows through microchannels. Exp Therm Fluid Sci 35:849–865

Sackmann J, Burlage K (2015) Review on ultrasonic fabrication of polymer micro devices. Ultrasonics 56:189–200

Salic A, Ana Tusek (2012) Application of microreactor in medicine and biomedicine. J Appl Biomed 10:137–153

Shojaeian M, Karimzadehkhouei M (2017) Experimental investigation on convective heat transfer of non-Newtonian flows of Xanthan gum solutions in microtubes. Exp Therm Fluid Sci 85:305–312

Singh RK, Kumar A (2014) Design and fabrication of 3-dimensional helical structures in polydimethylsiloxane for flow control applications. Microsyst Technol 20:101–111

Taylor JB, Carrano AL, Kandlikar SG (2006) Characterization of the effect of surface roughness and texture on fluid flow-past, present, and future. Int J Therm Sci 45:962–968

Wang QH, Zheng X (2011) Microtopographic modeling of three-dimension surface and simulation of flow characteristics of fluid in microchannels. J Central South Univ Technol 39:1–6

Wu WM, Manz A (2015) Rapid manufacture of modifiable 2.5-dimensional (2.5D) microstructures for capillary force-driven fluidic velocity control. RSC Adv 10:1039–1044

Yamada T, Hong C (2011) Experimental investigations of liquid flow in rib-patterned microchannels with different surface wettability. Microfluid Nanofluid 11:45–55

Yan H, Zhang WM (2015) Effect of random surface topography on the gaseous flow in microtubes with an extended slip model. Microfluid Nanofluid 18:897–910

Yeo LY, Chang H (2011) Microfluidic devices for bioapplications. Biomicrofluidics 7:12–48

Yuan X, Tao Z (2016) Experimental investigation of surface roughness effects on flow behavior and heat transfer characteristics for circular microchannels. Chin J Aeronaut 29:1575–1581

Zhang N, Gilchrist MD (2013) Characterization of microinjection molding process for milligram polymer microparts. Polymer Eng Sci 10:1458–1470

Zhang K, Zheng GH (2015) Experimental investigation on flow characteristics of gas in micro-channels. Proc Eng 99:758–762